CHEMISTRY OF MATERIALS
Communication
Cite This: Chem. Mater. 2019, 31, 3083−3088
pubs.acs.org/cm

$MnBi_2$: A Metastable High-Pressure Phase in the Mn−Bi System

James P. S. Walsh,[†] Samantha M. Clarke,[†,#] Danilo Puggioni,[∥] Alexandra D. Tamerius,[†] Yue Meng,[‡] James M. Rondinelli,[∥] Steven D. Jacobsen,[§] and Danna E. Freedman*,[†]

[†]Department of Chemistry, Northwestern University, Evanston, Illinois 60208, United States
[#]Physical and Life Sciences Directorate, Lawrence Livermore National Laboratory, Livermore, California 94550, United States
[∥]Department of Materials Science and Engineering, Northwestern University, Evanston, Illinois 60208, United States
[‡]HPCAT, X-Ray Science Division, Argonne National Laboratory, Argonne, Illinois 60439, United States
[§]Department of Earth and Planetary Sciences, Northwestern University, Evanston, Illinois 60208, United States

Supporting Information

Permanent magnetism underpins a wide range of applications including wind energy harvesting and electric powered vehicles, where magnets are a critical component of the generators and motors inherent to these technologies. Materials that fuse a large magnetic response with a high coercivity (i.e., resistance to demagnetization) display permanent magnetism. One approach toward creating novel permanent magnets is by bringing together atoms that are spin-bearing—featuring large magnetic moments—with atoms possessing significant orbital angular momentum, to induce a high coercivity. This strategy effectively recreates the magnetic structure of a lanthanide using two separately tunable species. Proof-of-concept for this approach resides in MnBi, a NiAs-type binary intermetallic compound first described in 1939,[1] which is a permanent magnet with remarkably competitive properties as compared to rare-earth magnets. Notably, in the 1950s, MnBi boasted the highest coercive force of any magnet known at the time. The peak value of 2.5 T for MnBi occurs at 523 K, because remarkably H_c rises with increasing temperature in this compound.[2−4] Although interest in MnBi waned upon the discovery in the 1960s of the first high-performance rare-earth magnets, $SmCo_5$[5] and Sm_2Co_{17},[6] this unusual material has nevertheless been investigated ever since due to its remarkable magnetic properties.[7−15] Indeed, the promise offered by MnBi, along with other rare-earth-free magnets such as the FePt class of alloys,[16,17] continues to drive fundamental magnetism research.

The early promising results within the Mn−Bi system suggest it merits further investigation, perhaps housing novel intermetallic phases with similarly exciting properties. Further, creating new phases within this space may enable a deeper understanding of the fundamental interactions between these two elements. To explore this system, we exploited high pressure as a synthetic vector, an approach that previously enabled the discovery of novel compounds in other binary bismuth systems such as Co−Bi,[18] Fe−Bi,[19] Ni−Bi,[20] and Cu−Bi.[21−23] Herein, we report the discovery of the metastable $MnBi_2$—a previously unknown binary phase in the Mn−Bi system—which we synthesized above pressures of 8.3(1) GPa. Preliminary calculations on this phase indicate it may be a permanent magnet with a magnetic anisotropy of 0.205 MJ/m^3 in favor of the ⟨100⟩ magnetization direction at 0 K.

The temperature−composition phase diagram for the Mn−Bi system was first mapped out over a hundred years ago.[24] Under ambient pressures there are only two thermodynamically stable intermetallic phases in this system: the MnBi (NiAs-type) compound introduced earlier and an orthorhombic manganese-rich derivative, $Mn_{1.08}Bi$.[25,26] We chose to investigate the Mn−Bi system at high pressures using the laser-heated diamond anvil cell (LH-DAC).

Static pressures on the order of gigapascals (GPa) are applied to a sample by placing it between the tips of two large single crystal diamond anvils that are subsequently driven together under high loads. To create a more uniform pressure at the sample, a gasket material is placed between the diamond tips and the sample is loaded along with a pressure transmitting medium into a circular sample space drilled through the center of the gasket. In our case, the pressure transmitting medium is single crystal MgO polished to a thickness of 5−10 μm. This choice of medium is ideal because MgO acts as a thermal insulator between the sample and the diamonds, with the added benefit of being optically transparent, chemically inert, and a good calibrant of pressure through its known equation-of-state, which relates cell volume to pressure.[27] We heat our sample while it is held under high pressure using infrared laser irradiation methods, wherein a high flux of incident photons is focused onto the sample from both sides of the cell, raising the temperature to thousands of degrees kelvin at a very localized region (laser fwhm is around 40 μm). A schematic of the experimental setup is given in the Supporting Information, and further details are available elsewhere.[28−30]

We pressed a single crystal of MnBi to a thickness of around 5−10 μm, loaded a small flake of this crushed polycrystalline material into the DAC sample space, and pressurized it to 8.3(1) GPa, as determined by the lattice parameters of the MgO pressure medium. X-ray diffraction data collected before heating exhibits peaks from MnBi, MgO, and Bi(V), which is the stable high-pressure polymorph of bismuth above 7.7 GPa.[31] The presence of elemental bismuth is due to the flux method used to prepare the MnBi sample.[32] Even before heating, we observed the appearance of peaks that had arisen during compression that could not be attributed to MnBi,

Received: January 26, 2019
Revised: April 22, 2019
Published: April 24, 2019

DOI: 10.1021/acs.chemmater.9b00385
Chem. Mater. 2019, 31, 3083−3088

$Mn_{1.08}Bi$, or any of the known polymorphs of the pure elements.

Upon heating to temperatures of around 400−700 K, the intensity of the peaks from the unknown phase increased as a function of time, with a concomitant decrease in the intensity of peaks from the MnBi phase (Figure 1). Heating was stopped once the peaks from the new phase had ceased growing in intensity. A small amount of α-Mn and MnBi remained at the end of the heating, and the pressure had increased slightly to 8.7(1) GPa. The peaks from the new phase are readily indexed at this pressure to the $I4/mcm$ space group with unit cell parameters a = 6.8315(1) Å and c = 5.6572(2) Å. A common structure type in this space group is Al_2Cu, and indeed the pattern can be modeled very well using Rietveld methods as $MnBi_2$ in this structure type (Figure 2). The reaction appears to proceed by the decomposition of MnBi (2MnBi → $MnBi_2$ + Mn), as evidenced by the very small amount of Bi present before the reaction, which would otherwise limit the alternative "bismuth uptake" mechanism (MnBi + Bi → $MnBi_2$). $MnBi_2$ can also be synthesized from a mixture of the elements, albeit in lower yields (Supporting Information).

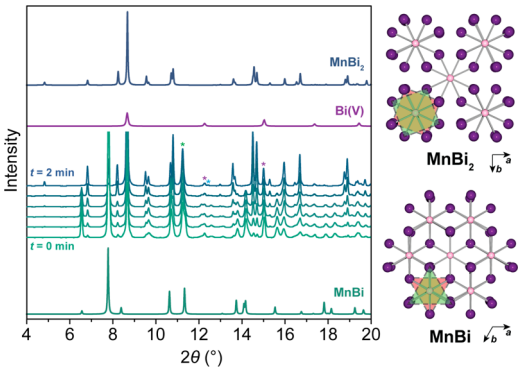

Figure 1. Left: Powder X-ray diffraction patterns collected in situ over the course of 2 min during laser heating of a pressed flake of MnBi under a pressure of 8.3(1) GPa. Simulated patterns of MnBi, $MnBi_2$, and Bi(V) at the same pressure are shown for comparison. Green, purple, and blue asterisks mark the positions of the highest intensity peaks from MgO, Bi(V), and α-Mn, respectively. Temperature during heating was estimated to be between 400−700 K. Right: Comparison of the crystal structures of MnBi and $MnBi_2$ as viewed along the c-axis, highlighting the faces that are shared between neighboring Mn atoms to form columns throughout the structure (red/green polygons overlaid in the lower left of each structure).

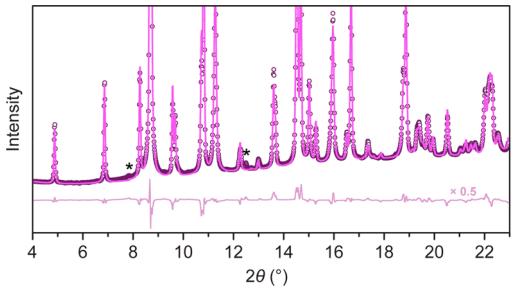

Figure 2. Rietveld refinement of the powder X-ray diffraction data collected at the conversion site after cooling to room temperature. Experimental data shown in black circles, fit shown as a purple line, and difference curve plotted in gray. The pressure at this site was 8.7(1) GPa. Asterisks mark the highest intensity peaks from the α-Mn (∼12.5°) and MnBi (∼8°) phases. Full details of the refinement are given in the Supporting Information. λ = 0.4066 Å. R_{wp} = 4.08.

The structure of $MnBi_2$ is analogous to that of $FeBi_2$, which also requires high pressure to form.[19] Each manganese atom is surrounded by eight bismuth atoms in a square antiprism coordination, with face-sharing of the squares between neighboring Mn sites leading to the formation of columns along the c-direction. Each column shares edges with its four surrounding columns throughout the ab-plane.

Both MnBi and $MnBi_2$ contain linear chains of Mn atoms that in each case define the long axis of face-sharing columns along the c-direction. In the case of MnBi, the Mn atoms are surrounded by six bismuth atoms in a triangular antiprism coordination environment, in contrast to the eight bismuth atoms in a square antiprism coordination in $MnBi_2$. The shortest Bi−Bi interaction in MnBi is 3.94 Å, which is clearly nonbonding; therefore, the Mn−Bi bond (2.77 Å) is the primary stabilizing influence on this structure. In contrast, $MnBi_2$ contains Bi−Bi interactions that are well below expected contact distances: at 8.7(1) GPa, the shortest Bi−Bi interactions, d_1 and d_2, are 3.101(1) Å and 3.316(1) Å ($2r_{Bi}$ = 3.38 Å). The Mn−Bi and Mn−Mn interactions at the same pressure are 2.930(1) Å and 2.829(1) Å, respectively. The comparison of these distances with the expected contact distance for the elements is consistent with what is generally observed for the Al_2Cu-type and implicates the Bi−Bi interactions as the primary stabilizing influence, with the Mn−Bi distance also being suggestive of a bonding interaction yet no interaction being observed between Mn atoms along the c-axis (vida infra and Supporting Information). Similarities between MnBi and $MnBi_2$ are clearly seen when both structures are viewed down the c-direction (Figure 1, right) and when compared side by side (Figure 3).

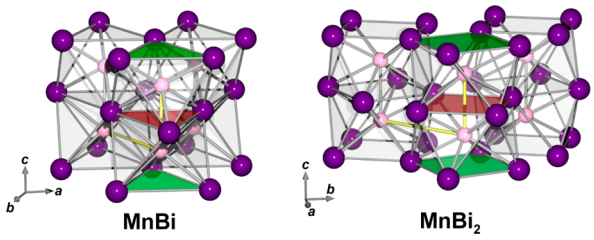

Figure 3. Comparison of the crystal structures of MnBi and $MnBi_2$, highlighting the formation of face-sharing columns along the c-direction that edge-share across the ab-plane. Faces that are shared between Mn coordination environments are highlighted in red/green, as in Figure 1. Mn and Bi atoms are represented by pink and purple spheres, respectively. Yellow rods highlight the two nearest-neighbor Mn−Mn magnetic interactions: J_{in} (in the ab-plane) and J_{out} (along the c-axis).

We investigated the electronic structure of $MnBi_2$ at 8.7(1) GPa using density functional theory (DFT) calculations performed on the experimentally determined structure. The top panel of Figure 4 shows the electronic projected density-of-states (DOS) of nonmagnetic (NM) $MnBi_2$. The region near the Fermi level (E_F) is populated by Bi 6p and Mn 3d electrons. The Bi 6s electrons are at lower energies (around 9 to 12 eV below E_F). This distribution of states is qualitatively very similar to those calculated previously for MnBi,[33,34] where the Mn 3d and Bi 6p states dominate the region close to the Fermi energy and the Bi 6s states are similarly isolated at 10 to 12 eV below E_F. For both MnBi and $MnBi_2$, the calculated

DOI: 10.1021/acs.chemmater.9b00385
Chem. Mater. 2019, 31, 3083−3088

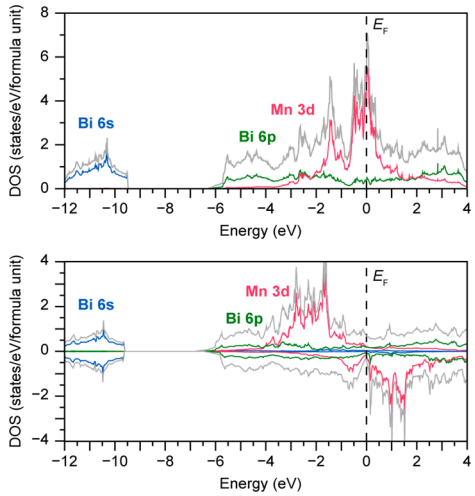

Figure 4. Projected density of states (DOS) per formula unit for the nonmagnetic (top panel) and ferromagnetic (bottom panel) ground state of $MnBi_2$ calculated within DFT-PBEsol. Energies are given relative to the Fermi level (vertical dashed line). Contributions from individual orbitals are plotted in different colors, while the total DOS is plotted in gray.

DOS is consistent with strong covalent Mn−Bi interactions, where hybridization between the Mn 3d and Bi 6p states leads to electron delocalization. The total DOS at E_F is about 6.3 states/eV/f.u., with a Van Hove singularity located ∼20 meV above E_F. Within Stoner theory,[35] a ferromagnetic instability is expected when $NI > 1$, where N is the number of states at E_F and I are the Stoner parameters. Since the DOS at E_F is dominated by Mn states, it is appropriate to choose $I = 0.4$ eV,[36] which puts $MnBi_2$ on the verge of a magnetic instability.

To evaluate the magnetic ground state of $MnBi_2$, we include the spin degree of freedom in our calculation (see Supporting Information for details). We find that $MnBi_2$ exhibits local magnetic moments of ∼3.2 μ_B at the Mn sites and ∼0.07 μ_B at the Bi sites,[37] the magnetic moments at the Mn sites are aligned ferromagnetically with each other, while the magnetic moments at the Bi sites are aligned antiferromagnetically to the Mn sites due to the strong Mn 3d−Bi 6p hybridization.[38] This coupling scheme is strikingly similar to that exhibited by MnBi, for which an earlier theoretical work suggested magnetic moments in the range of 3.57−3.68 μ_B for Mn and 0.06−0.08 μ_B for Bi.[38,39] The projected DOS for this magnetic configuration is given in the bottom panel of Figure 4.

We calculate the first excited state in $MnBi_2$ to have antiferromagnetic Mn−Mn interactions, with a total energy that is 69 meV/f.u. higher than the ferromagnetic ground state. To estimate the exchange integrals (J_i), we calculated the total energy difference between the ground and excited state magnetic configurations,[40] assuming the $-JS_i \cdot S_j$ convention in the Heisenberg spin Hamiltonian. We found that the in-plane and out-of-plane exchange integrals are both ferromagnetic, with values of 3.4 and 23.5 meV, respectively. We also calculated the Curie temperature, T_C, using the following mean field approximation:

$$T_C = \frac{2\gamma}{3k_B}\sum_1 J_i \qquad (1)$$

where k_B is the Boltzmann constant and the factor γ is given by $S(S + 1)/S^2$ for quantum spins ($\gamma = 1$ for classical spins).[41] Assuming a quantum spin ($S = 3/2$, $\gamma = 5/3$), we find $T_C = 521$ K, which is comparable with the experimental value of 628 K measured for MnBi.[42] For classical spins, T_C is reduced to 208 K.

A critical property of permanent magnets is their coercivity, which is derived in large part from the magnetocrystalline anisotropy energy; the greater this energy, the stronger the preference for the material to align its magnetism along a specific direction. Given the remarkable magnetic properties of MnBi, which are derived in large part from its unusual property of exhibiting an increased coercivity at elevated temperatures,[26] we also examine the magnetocrystalline anisotropy of $MnBi_2$.

We calculated the DOS with the magnetization aligned along the ⟨100⟩ and ⟨001⟩ directions, with the spin−orbit interaction (SOI) included (see Supporting Information). Although the spin−orbit interaction mixes the up- and down-spin channels, the DOS are qualitatively similar to the non-SOI calculation shown in Figure 4. Comparing the DOS for the ⟨001⟩ and ⟨100⟩ magnetization directions, we note that the former exhibits a strong degeneracy at around −4.0 and +2.0 eV relative to E_F that is not present in the ⟨100⟩ case (compare insets in Figure S5). Although subtle, this difference in degeneracy results in a magnetocrystalline anisotropy energy of 0.205 MJ/m^3 (or 0.338 meV per formula unit) in favor of the ⟨100⟩ magnetization direction. This is comparable to the value of 0.275 MJ/m^3 predicted for MnBi.[39] Our efforts to isolate $MnBi_2$ in bulk form will support the study of magnetism in this remarkable new material.

Currently, attempts to recover $MnBi_2$ to ambient pressures were unsuccessful, with complete loss of diffraction peaks upon completely releasing the load on the diamond anvils (see Supporting Information). Diffraction peaks from the $MnBi_2$ phase are lost below approximately 3−4 GPa. Peaks from the MnBi phase grow in intensity over the course of the decompression, indicating that $MnBi_2$ decomposes by the expulsion of bismuth atoms, perhaps to reduce the Mn coordination from the increasingly unfavorable eight-coordinate to six-coordinate as the relative atomic radius of Bi versus Mn (r_{Bi}/r_{Mn}) increases. Diffraction peaks from bismuth are also observed to grow alongside those from MnBi, consistent with the difference in stoichiometry between the two phases. A similar lack of quenchability is also observed in $FeBi_2$, which is detectable only down to around 3 GPa.[19]

$MnBi_2$ and $FeBi_2$ are currently the only known examples of bismuthides crystallizing in the Al_2Cu structure type, and both appear to be unstable at ambient pressure (i.e., metastable). This observation led us to examine why $MnBi_2$ does not lend itself to recovery to ambient conditions, with a view to inspire approaches for future work targeting its recovery.

We repeated the synthesis of $MnBi_2$ starting from a higher pressure (10.5(1) GPa) so that we could collect decompression data over a wider range of pressures. During this synthesis, the pressure had increased to 11.7(1) GPa after the reaction. Aided by the crystallographic simplicity of the structure, we are able to use Rietveld methods to reliably extract the Wyckoff 8*h* *x*-coordinate from the data collected during decompression, which in turn allows us to calculate interatomic distances reliably as a function of pressure. The salient interactions we extract are the Mn−Mn, the Mn−Bi, and the shortest and second shortest Bi−Bi interactions, which we denote as d_1 and d_2, respectively. Selected crystallographic parameters for the highest and lowest pressures measured for $MnBi_2$ are given in Table 1 for comparison.

DOI: 10.1021/acs.chemmater.9b00385
Chem. Mater. 2019, 31, 3083−3088

Table 1. Selected Crystallographic Parameters for $MnBi_2$ at the Highest and Lowest Pressures Measured in This Study

	$MnBi_2$ (11.7 GPa)	$MnBi_2$ (3.7 GPa)
a	6.7292(4) Å	6.976(1) Å
c	5.5825(5) Å	5.735(1) Å
c/a	0.8296	0.822
x	0.1609(4)	0.1591(6)
Mn−Mn	2.7912(3) Å	2.8673(7) Å
Mn−Bi	2.890(2) Å	2.990(4) Å
Bi−Bi (d_1)	3.034(5) Å	3.138(8) Å
Bi−Bi (d_2)	3.281(3) Å	3.383(5) Å
d_1/d_2	0.925	0.928

We performed two empirical analyses on the structure of $MnBi_2$ as a function of pressure, the full details of which can be found in the Supporting Information. In our first analysis, we examined the d_1 and d_2 interactions. We found that d_1 remains below the expected bonding threshold for a Bi−Bi interaction over all pressures. However, below ∼6 GPa, d_2 begins to rapidly approach this limit with a projected intercept at around ∼3 GPa, indicating that this bond breaks during decompression (Figure 5, top).

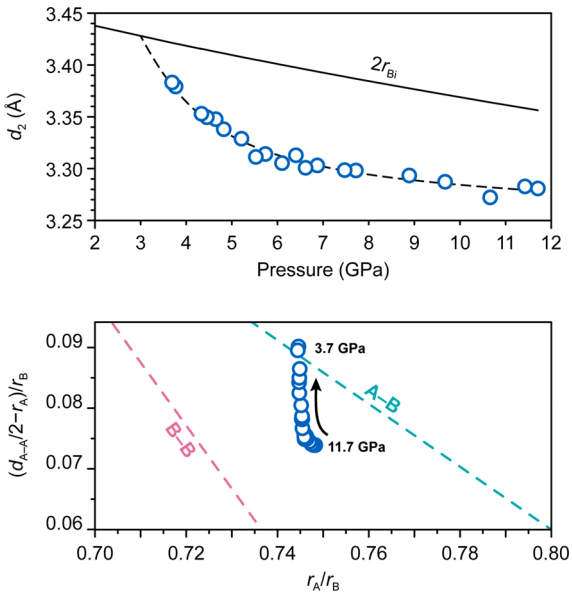

Figure 5. Top: Plot of d_2, the second shortest Bi−Bi interaction in $MnBi_2$, as a function of pressure. Solid line shows the expected bonding interaction for 15-coordinate Bi as a function of pressure. Dashed line is a guide for the eye. Bottom: Nearest neighbor diagram for Al_2Cu-type compounds. Values have been corrected to remove dependence of the A−B and B−B lines on the c/a ratio, following ref 43. Data points are plotted for the $MnBi_2$ structures determined over decompression from 11.7 GPa until 3.7 GPa, below which the sample decomposed fully into MnBi and Bi.

In our second analysis, we examined the subtle variation in the structure adopted by $MnBi_2$ as a function of decompression by plotting it within a nearest-neighbor diagram previously established for the Al_2Cu structure type (Figure 5, bottom).[43] This analysis shows that while at high pressure $MnBi_2$ adopts a structure that is well within the Al_2Cu-type stability field, it begins to distort below ∼6 GPa in such a way that by the lowest pressures (∼3 GPa) the Mn−Bi distance becomes unfavorably long for a bonding interaction.

Taken together, the two analyses implicate structural distortion as the primary cause for decomposition of $MnBi_2$ at low pressures. While the Al_2Cu type is easily adopted under compression—where the r_{Mn}/r_{Bi} ratio has become favorable—as pressure is released and r_{Bi} expands more rapidly than r_{Mn}, this ratio becomes too small and the Al_2Cu structure is no longer structurally stable. Although this result may seem intuitive from the size difference of the two elements, quantification is nevertheless important for determining approaches toward the ambient-pressure stabilization of exotic high-pressure phases. From the present results, it appears that a control of r_A/r_B using chemical site doping at the B site could be a promising direction to pursue.

We reported the discovery of $MnBi_2$, a new metastable intermetallic phase in the Mn−Bi system. This compound bears strong structural similarities to MnBi, which makes it a promising compound for further experimental study in search of outstanding magnetic properties. We examined the structure as a function of decompression in order to understand why it does not survive to ambient pressure and found that the unfavorable r_{Mn}/r_{Bi} ratio is likely to be the primary cause for the loss of structural stability at low pressures. Preliminary studies of the electronic and magnetic structure of $MnBi_2$ using DFT show that it shares many features with MnBi, such as strong covalent interactions between Mn and Bi, as well as a ferromagnetic alignment of the magnetic moments on the Mn sites. We also find the magnetocrystalline anisotropy to be comparable with that found in MnBi. Future work will explore in situ approaches for the characterization of $MnBi_2$ under high pressures, alongside attempts to recover samples to ambient pressure through the use of chemical site doping.

■ ASSOCIATED CONTENT

Supporting Information

The Supporting Information is available free of charge on the ACS Publications website at DOI: 10.1021/acs.chemmater.9b00385.

Crystallographic information file (CIF)

Additional synthesis details, crystallographic refinement parameters, and details for DFT calculations (PDF)

■ AUTHOR INFORMATION

Corresponding Author

*E-mail: danna.freedman@northwestern.edu.

ORCID

James M. Rondinelli: 0000-0003-0508-2175

Steven D. Jacobsen: 0000-0002-9746-958X

Danna E. Freedman: 0000-0002-2579-8835

Funding

This research was initiated with funding from AFOSR (FA9550-14-1-0358, FA9550-17-1-0247), and funding from DOE (DE-SC0018092) supported work on decompression. J.P.S.W. was supported by the Innovative Initiatives Incubator (I3) at Northwestern University. S.M.C. acknowledges support from the NSF GRFP (DGE-1324585). Part of this work was performed under the auspices of the U.S. Department of Energy by Lawrence Livermore National Security, LLC, under Contract DE-AC52-07NA27344. This work was performed at HPCAT (Sector 16), Advanced Photon Source (APS), Argonne National Laboratory. HPCAT operations are supported by DOE-NNSA's Office of Experimental Sciences.

DOI: 10.1021/acs.chemmater.9b00385
Chem. Mater. 2019, 31, 3083−3088

Additional beamtime support was provided by the Capital/DOE Alliance Center (CDAC). The Advanced Photon Source is a U.S. Department of Energy (DOE) Office of Science User Facility operated for the DOE Office of Science by Argonne National Laboratory under Contract No. DE-AC02-06CH11357. D.P. and J.M.R. acknowledge the Army Research Office under Grant No. W911NF-15-1-0017 and the DOD-HPCMP for computational resources.

Notes

The authors declare no competing financial interest.

■ REFERENCES

(1) Hocart, R.; Guillaud, C. *C. R. Acad. Sc.* **1939**, *209*, 443.
(2) Bismanol: NOL Develops New Magnetic Material. *Phys. Today* **1952**, *5* (8), 19.
(3) Adams, E.; Hubbard, W. M.; Syeles, A. M. A new permanent magnet from powdered manganese bismuthide. *J. Appl. Phys.* **1952**, *23*, 1207−1211.
(4) Yang, Y.; Chen, X.; Guo, S.; Yan, A.; Huang, Q.; Wu, M.; Chen, D.; Yang, Y.; Yang, J. Temperature dependences of structure and coercivity for melt-spun MnBi compound. *J. Magn. Magn. Mater.* **2013**, *330*, 106−110.
(5) Strnat, K.; Hoffer, G.; Olson, J.; Ostertag, W.; Becker, J. A family of new cobalt-base permanent magnet materials. *J. Appl. Phys.* **1967**, *38*, 1001−1002.
(6) Strnat, K.; Hoffer, G.; Ostertag, W.; Olson, J. Ferrimagnetism of the rare-earth-cobalt intermetallic compounds R_2Co_{17}. *J. Appl. Phys.* **1966**, *37*, 1252−1253.
(7) Guillaud, C. Polymorphisme du composé défini Mn−Bi aux températures de disparition et de réapparition de l'aimantation spontanée. *J. Phys. Radium* **1951**, *12*, 143.
(8) Heikes, R. R. Magnetic Transformation in MnBi. *Phys. Rev.* **1955**, *99*, 446−447.
(9) Roberts, B. W. Neutron diffraction study of the structures and magnetic properties of manganese bismuthide. *Phys. Rev.* **1956**, *104*, 607−616.
(10) Andresen, A.; Hälg, W.; Fischer, P.; Stoll, E.; Eriksson, G.; Blinc, R.; Paušak, S.; Ehrenberg, L.; Dumanović, J. The magnetic and crystallographic properties of MnBi studied by neutron diffraction. *Acta Chem. Scand.* **1967**, *21*, 1543.
(11) Andresen, A.; Engebretsen, J.; Refsnes, J.; Huhtikangas, A.; Pearson, W. B.; Meisalo, V. Neutron-diffraction Investigations on Quenched MnBi and $MnBi_{0.9}Sb_{0.1}$. *Acta Chem. Scand.* **1972**, *26*, 175−190.
(12) Di, G.; Iwata, S.; Tsunashima, S.; Uchiyama, S. Magneto-optical kerr effects of MnBi and MnBiAl films. *J. Magn. Magn. Mater.* **1992**, *104*, 1023−1024.
(13) Yang, J.; Kamaraju, K.; Yelon, W. B.; James, W. J.; Cai, Q.; Bollero, A. Magnetic properties of the MnBi intermetallic compound. *Appl. Phys. Lett.* **2001**, *79*, 1846−1848.
(14) Antropov, V.; Antonov, V.; Bekenov, L.; Kutepov, A.; Kotliar, G. Magnetic anisotropic effects and electronic correlations in MnBi ferromagnet. *Phys. Rev. B: Condens. Matter Mater. Phys.* **2014**, *90*, 054404.
(15) Williams, T.; Taylor, A.; Christianson, A.; Hahn, S.; Fishman, R.; Parker, D.; McGuire, M.; Sales, B.; Lumsden, M. Extended magnetic exchange interactions in the high-temperature ferromagnet MnBi. *Appl. Phys. Lett.* **2016**, *108*, 192403.
(16) Klemmer, T.; Hoydick, D.; Okumura, H.; Zhang, B.; Soffa, W. Magnetic hardening and coercivity mechanisms in $L1_0$ ordered FePd ferromagnets. *Scr. Metall. Mater.* **1995**, *33*, 1793−1805.
(17) Gutfleisch, O.; Lyubina, J.; Müller, K.-H.; Schultz, L. FePt hard magnets. *Adv. Eng. Mater.* **2005**, *7*, 208−212.
(18) Schwarz, U.; Tencé, S.; Janson, O.; Koz, C.; Krellner, C.; Burkhardt, U.; Rosner, H.; Steglich, F.; Grin, Y. $CoBi_3$: A binary cobalt−bismuth compound and superconductor. *Angew. Chem., Int. Ed.* **2013**, *52*, 9853−9857.
(19) Walsh, J. P. S.; Clarke, S. M.; Meng, Y.; Jacobsen, S. D.; Freedman, D. E. Discovery of $FeBi_2$. *ACS Cent. Sci.* **2016**, *2*, 867−871.
(20) Powderly, K. M.; Clarke, S. M.; Amsler, M.; Wolverton, C.; Malliakas, C. D.; Meng, Y.; Jacobsen, S. D.; Freedman, D. E. High-Pressure Discovery of β-NiBi. *Chem. Commun.* **2017**, *53*, 11241−11244.
(21) Clarke, S. M.; Walsh, J. P. S.; Amsler, M.; Malliakas, C. D.; Yu, T.; Goedecker, S.; Wang, Y.; Wolverton, C.; Freedman, D. E. Discovery of a Superconducting Cu−Bi Intermetallic Compound by High-Pressure Synthesis. *Angew. Chem., Int. Ed.* **2016**, *55*, 13446−13449.
(22) Guo, K.; Akselrud, L.; Bobnar, M.; Burkhardt, U.; Schmidt, M.; Zhao, J.-T.; Schwarz, U.; Grin, Y. Weak Interactions under Pressure: *hp*-CuBi and Its Analogues. *Angew. Chem., Int. Ed.* **2017**, *56*, 5620−5624.
(23) Clarke, S. M.; Amsler, M.; Walsh, J. P. S.; Yu, T.; Wang, Y.; Meng, Y.; Jacobsen, S. D.; Wolverton, C.; Freedman, D. E. Creating Binary Cu−Bi Compounds via High-Pressure Synthesis: A Combined Experimental and Theoretical Study. *Chem. Mater.* **2017**, *29*, 5276−5285.
(24) Parravano, N.; Perret, U. Sulle leghe di manganese e bismuto. *Gazz. Chim. Ital.* **1915**, *45*, 390−394.
(25) Chen, T. Contribution to the equilibrium phase diagram of the Mn−Bi system near MnBi. *J. Appl. Phys.* **1974**, *45*, 2358−2360.
(26) Chen, T.; Stutius, W. The phase transformation and physical properties of the MnBi and $Mn_{1.08}Bi$ compounds. *IEEE Trans. Magn.* **1974**, *10*, 581−586.
(27) Speziale, S.; Zha, C.-S.; Duffy, T. S.; Hemley, R. J.; Mao, H.-k. Quasi-hydrostatic compression of magnesium oxide to 52 GPa: Implications for the pressure-volume-temperature equation of state. *J. Geophys. Res.: Solid Earth* **2001**, *106*, 515−528.
(28) Meng, Y.; Shen, G.; Mao, H. Double-Sided Laser Heating System at HPCAT for In Situ X-ray Diffraction at High Pressures and High Temperatures. *J. Phys.: Condens. Matter* **2006**, *18*, S1097.
(29) Meng, Y.; Hrubiak, R.; Rod, E.; Boehler, R.; Shen, G. New Developments in Laser-Heated Diamond Anvil Cell with In Situ Synchrotron X-ray Diffraction at High Pressure Collaborative Access Team. *Rev. Sci. Instrum.* **2015**, *86*, 072201.
(30) Walsh, J. P. S.; Freedman, D. E. High-Pressure Synthesis: A New Frontier in the Search for Next-Generation Intermetallic Compounds. *Acc. Chem. Res.* **2018**, *51*, 1315−1323.
(31) Akahama, Y.; Kawamura, H.; Singh, A. K. Equation of state of bismuth to 222 GPa and comparison of gold and platinum pressure scales to 145 GPa. *J. Appl. Phys.* **2002**, *92*, 5892−5897.
(32) McGuire, M. A.; Cao, H.; Chakoumakos, B. C.; Sales, B. C. Symmetry-lowering lattice distortion at the spin reorientation in MnBi single crystals. *Phys. Rev. B: Condens. Matter Mater. Phys.* **2014**, *90*, 174425.
(33) Coehoorn, R.; de Groot, R. A. The electronic structure of MnBi. *J. Phys. F: Met. Phys.* **1985**, *15*, 2135−2144.
(34) Park, J.; Hong, Y.-K.; Lee, J.; Lee, W.; Kim, S.-G.; Choi, C.-J. Electronic Structure and Maximum Energy Product of MnBi. *Metals* **2014**, *4*, 455−464.
(35) Blundell, S. J. *Magnetism in Condensed Matter*; Oxford University Press: Oxford, U.K., 2001.
(36) Sigalas, M.; Papaconstantopoulos, D. Calculations of the total energy, electron-phonon interaction, and Stoner parameter for metals. *Phys. Rev. B: Condens. Matter Mater. Phys.* **1994**, *50*, 7255.
(37) Podloucky, R.; Redinger, J. Density functional theory study of structural and thermodynamical stabilities of ferromagnetic MnX (X= P, As, Sb, Bi) compounds. *J. Phys.: Condens. Matter* **2019**, *31*, 054001.
(38) Coehoorn, R.; de Groot, R. A. The electronic structure of MnBi. *J. Phys. F: Met. Phys.* **1985**, *15*, 2135−2144.
(39) Park, J.; Hong, Y.-K.; Lee, J.; Lee, W.; Kim, S.-G.; Choi, C.-J. Electronic Structure and Maximum Energy Product of MnBi. *Metals* **2014**, *4*, 455−464.
(40) Lampis, N.; Franchini, C.; Satta, G.; Geddo-Lehmann, A.; Massidda, S. Electronic structure of $PbFe_{1/2}Ta_{1/2}O_3$: Crystallographic

DOI: 10.1021/acs.chemmater.9b00385
Chem. Mater. 2019, 31, 3083−3088

ordering and magnetic properties. *Phys. Rev. B: Condens. Matter Mater. Phys.* **2004**, *69*, 064412.
(41) MacLaren, J. M.; Schulthess, T. C.; Butler, W. H.; Sutton, R.; McHenry, M. Electronic structure, exchange interactions, and Curie temperature of FeCo. *J. Appl. Phys.* **1999**, *85*, 4833.
(42) Chen, T.; Stutius, W. The phase transformation and physical properties of the MnBi and Mn 1.08 Bi compounds. *IEEE Trans. Magn.* **1974**, *10*, 581−586.
(43) Havinga, E. E.; Damsma, H. Compounds and pseudo-binary alloys with the $CuAl_2$(C16)-type structure III. Stability and competitive structures. *J. Less-Common Met.* **1972**, *27*, 269−280.

DOI: 10.1021/acs.chemmater.9b00385
Chem. Mater. 2019, 31, 3083−3088